

The Red Giant Branch Tip and Bump of the Leo II dwarf spheroidal galaxy

M. Bellazzini¹, N. Gennari², F.R. Ferraro² *

¹INAF - Osservatorio Astronomico di Bologna, via Ranzani 1, 40127, Bologna, Italy

²Università di Bologna - Dipartimento di Astronomia, via Ranzani 1, 40127, Bologna, Italy

19 November 2018

ABSTRACT

We present V and I photometry of a $9.4' \times 9.4'$ field centered on the dwarf spheroidal galaxy Leo II. The Tip of the Red Giant Branch is identified at $I^{TRGB} = 17.83 \pm 0.03$ and adopting $\langle [M/H] \rangle = -1.53 \pm 0.2$ from the comparison of RGB stars with Galactic templates, we obtain a distance modulus $(m - M)_0 = 21.84 \pm 0.13$, corresponding to a distance $D = 233 \pm 15$ Kpc. Two significant bumps have been detected in the Luminosity Function of the Red Giant Branch. The fainter bump (B1, at $V = 21.76 \pm 0.05$) is the RGB bump of the dominant stellar population while the actual nature of the brightest one (B2, at $V = 21.35 \pm 0.05$) cannot be firmly assessed on the basis of the available data, it can be due to the Asymptotic Giant Branch Clump of the main population or it may be a secondary RGB bump. The luminosity of the main RGB bump (B1) suggests that the majority of RGB stars in Leo II belongs to a population that is $\gtrsim 4$ Gyr younger than the classical Galactic globular clusters. The stars belonging to the He-burning Red Clump are shown to be significantly more centrally concentrated than RR Lyrae and Blue Horizontal Branch stars, probing the existence of an age/metallicity radial gradient in this remote dwarf spheroidal.

Key words: stars: Population II - galaxies: distances and redshifts - Local Group - variable stars: RR Lyrae

1 INTRODUCTION

Leo II (Harrington & Wilson 1950) is one of the most distant dwarf spheroidal (dSph) satellites of the Milky Way ($D \simeq 205$ Kpc, according to Mateo 1998). From deep HST photometry Mighell & Rich (1996) determined a mean age of 9 ± 1 Gyr for the main stellar population of this galaxy, with a Star Formation History (SFH) started ~ 14 Gyr ago and lasted for ~ 7 Gyr. According to these authors, after this epoch the SF in Leo II has been very low and, at most, sporadic (see also Bosler et al. 2004, that reached similar conclusions following a different path). The presence of a significant fraction of old stars (e.g., age $\gtrsim 10$ Gyr) in this galaxy is witnessed by a conspicuous population of RR Lyrae variables (see Siegel & Majewski 2000, and references therein) and Blue Horizontal Branch (BHB) stars (Demers & Irwin 1993; Mighell & Rich 1996).

The observed color of the Red Giant Branch (RGB) is typical of a metal poor population, and most of the existing photometric studies (Demers & Harris 1983; Lee 1995; Demers & Irwin 1993) agree in deriving an average metallicity $[Fe/H] \simeq -1.9$ in the Zinn & West (1984, hereafter ZW)

metallicity scale, with a metallicity dispersion of ~ 0.3 dex, while Mighell & Rich (1996) obtained $[Fe/H] \simeq -1.6$. During a recent low-resolution spectroscopic survey, Bosler et al. (2004) determined the metallicity of 41 RGB stars in Leo II, in the Carretta & Gratton (1997, hereafter CG) metallicity scale. The metallicity of the stars studied by Bosler et al. (2004) ranges from $[Fe/H]_{CG} = -2.32$ to $[Fe/H]_{CG} = -1.26$; the average metallicity is $\langle [Fe/H]_{CG} \rangle = -1.57$, in good agreement with the photometric estimates described above, once the differences in the metallicity scales are taken into account. A global mass-to-light ratio $M/L \simeq 11.1 \pm 3.8$ (Vogt et al. 1995) suggests that the Dark Matter (DM) is the main contributor to the total mass of the galaxy, as in most of the other dSphs of the Local Group.

As a part of a large programme aimed at obtaining homogeneous distances for most of the galaxies of the Local Group (see Bellazzini et al. 2002; Galletti, Bellazzini & Ferraro 2004; Bellazzini et al. 2004b; Monaco et al. 2004), we present here the results of the V,I photometry (reaching $V \simeq 23$) of a $9.4' \times 9.4'$ field centered on Leo II. We provide a new estimate of the distance to this galaxy using the Tip of the Red Giant Branch (TRGB) as a standard candle (see Lee et al. 1993a; Sakai, Madore & Freedman 1996;

* E-mail: bellazzini, ferraro@bo.astro.it

Madore & Freedman 1998; Salaris, Cassisi & Weiss 2003; Bellazzini, Ferraro & Pancino 2001; Bellazzini et al. 2004a, for details and references about the method), and we study the main properties of the evolved stellar populations of the galaxy. In the present analysis we consider a field of view significantly larger than in previous studies. Adopting a King profile for the light distribution of Leo II, with core radius $r_c = 2.9'$ and tidal radius $r_t = 8.7'$ (according to Mateo 1998), we estimate that our field cover a fraction of the area of the galaxy ($\simeq 37\%$) that includes more than 87% of the total integrated light emitted by Leo II. The corresponding figures (fraction of the area/fraction of the light) for previous studies are : 20%/70% (Demers & Irwin 1993), 16.6%/63% (Lee 1995), 11%/50% (Demers & Harris 1983), 2%/15% (Mighell & Rich 1996). The larger radial range explored by the present study may be at the origin of some differences in the estimates of the average properties of the galaxy (as, for example the mean metallicity) with respect to previous analyses, due to radial population gradients (see Sect. 3.2 and 5., below).

The plan of the paper is the following: in Sect. 2 we describe the observational material, the data reduction process, the artificial stars experiments, we briefly discuss the Color Magnitude Diagrams and we present the light-curve of a newly identified variable; in Sect. 3 we report on the detection of the TRGB, and on our estimate of the distance modulus. In Sect. 4 we discuss the two bumps we identify in the Luminosity Function of the RGB and in Sect. 5 we present and discuss the radial distribution of HB stars, showing the presence of a population gradient. Finally, the main results are summarized in Sect. 6.

2 OBSERVATIONS, DATA REDUCTION AND COLOR MAGNITUDE DIAGRAMS

The data were obtained at the 3.52 *m* Italian telescope TNG (Telescopio Nazionale Galileo - Roque de los Muchachos, La Palma, Canary Islands, Spain), using DoLoRes, a focal reducer imager/spectrograph equipped with a 2048×2048 pixels CCD array. The pixel scale is 0.275 arcsec/px. The observations were carried out during three nights (March 19, 20 and 21, 2001), under average seeing conditions ($FWHM \simeq 1.0'' - 1.4''$). The data have been acquired during the same observational run already described in Bellazzini et al. (2002, 2004b): any further detail may be found in those papers.

We acquired five exposures in I (two with $t_{exp} = 600$ s, and three with $t_{exp} = 300$ s), and eight exposures in V (two with $t_{exp} = 600$ s, and six with $t_{exp} = 300$ s), centered on the center of Leo II. All the raw images were corrected for bias and flat field, and the overscan region was trimmed using standard IRAF¹ procedures. Each set of images was registered, flux-normalized and combined into one single *master frame* (per filter) using the tasks *interp.csh* and *ref.csh* of the

ISIS-2.1 package (Alard 1999). ISIS is able to combine images into a master frame having the seeing of the best image in the set, without any loss of flux (Alard 1999, 2000)².

The PSF-fitting procedure was performed independently on each V and I master image, using a version of DoPhot (Schechter, Mateo & Saha 1992) modified by P. Montegriffo at the Bologna Observatory to read images in double precision format. The frames were searched for sources adopting a $5\text{-}\sigma$ threshold, and the spatial variations of the PSF were modeled with a quadratic polynomial. The adopted threshold corresponds to the limiting magnitudes $I \simeq 22.2$ and $V \simeq 23.2$. A final catalogue listing the instrumental V,I magnitudes for all the stars in each field has been obtained by cross-correlating the V and I catalogues. Only the sources classified as stars by the code have been retained. Aperture corrections have been determined on a sample of bright and isolated stars in each of the master frames and applied to the catalogues.

The transformation to the standard Johnson-Cousins photometric system has been achieved using the calibrating relation obtained and described in Bellazzini et al. (2002). The absolute calibration has been checked against independent photometries (Stetson 2000; Momany 2000) and it has been found to be accurate at the ± 0.02 mag level (see Bellazzini et al. 2002). The astrometric solution to transform the original reference frame (X,Y in pixels) to equatorial coordinates at the 2000.0 Equinox have been obtained from 58 stars in common with the GSC2.2 catalogue³, using a dedicated package developed by P. Montegriffo at the Bologna Observatory. The root-mean-square residuals of the transformation are $< 0.2''$ in both RA and Dec.

We cross-correlated our catalog with the Near Infrared Point Source Catalogue of 2MASS (Cutri et al. 2003) and we found 18 sources in common, among the brightest and reddest stars of our dataset. The root-mean-square between our astrometric solution and the astrometry from 2MASS for the 18 stars in common is $< 0.15''$ in both RA and Dec. We identified also 5 carbon stars from Azzopardi, Lequeux & Westerlund (1985) and 111 RR Lyrae and 2 anomalous cepheids from the catalog of Siegel & Majewski (2000). The final catalogue is available in electronic form from the CDS.

$E(B-V) = 0.02 \pm 0.01$, according to Mateo (1998) (and in agreement with Schlegel, Finkbeiner & Davis 1998) and $A_I = 1.76E(B-V)$, according to Dean, Warren & Cousins (1978), are adopted throughout the following analysis.

2.1 Color-Magnitude Diagram

The Color Magnitude Diagram (CMD) obtained from our catalogue is displayed in Fig. 1. The morphology of the CMD is fully consistent with those presented and described in previous studies that attained sufficiently deep and accurate photometry to unveil the morphology of the entire Horizontal Branch (Demers & Irwin 1993; Mighell & Rich 1996; Momany 2000).

The CMD is dominated by the steep RGB of Leo II

¹ IRAF is distributed by the National Optical Astronomy Observatory, which is operated by the Association of Universities for Research in Astronomy, Inc., under cooperative agreement with the National Science Foundation.

² See also the on-line tutorial <http://www2.iap.fr/users/alard/tut.html>

³ see <http://www-gss.stsci.edu/gsc/gsc2/GSC2home.htm>

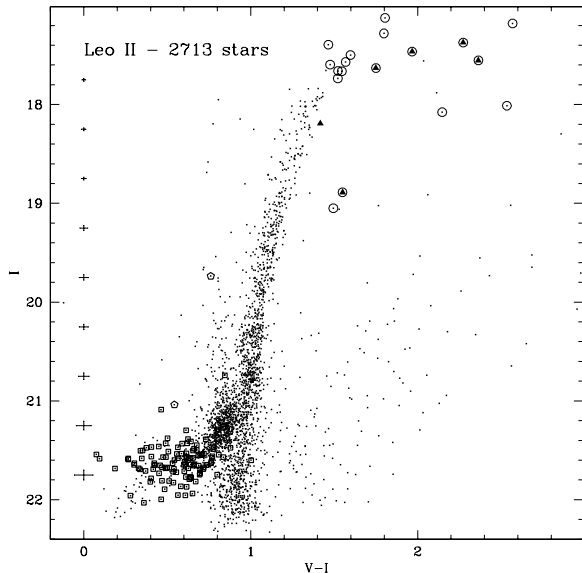


Figure 1. I,V-I CMD of Leo II. The characteristic photometric uncertainties are plotted in the two panels as errorbars aligned at $V - I = 0.0$. Large open circles mark stars in common with the Point Source Catalogue of 2MASS. Filled triangles are carbon stars we have identified from Azzopardi, Lequeux & Westerlund (1985). Pentagons are anomalous Cepheid (V53 and V171) and open squares are RR Lyrae identified from Siegel & Majewski (2000).

extending from the limiting magnitude to $I \simeq 17.8$. A handful of bright AGB stars, most of which are also detected in the infrared by 2MASS (marked by open circles in Fig. 1), are also present at $I < 18.0$ and $V - I \geq 1.4$. Most of the identified carbon stars are included in this family. The star detected by 2MASS at $I \simeq 19.0$ and $V - I \simeq 1.4$ may be an unknown carbon star but a check of the membership should be performed to obtain a firm classification. This star has $J - K \simeq 1.2$, similar to that of the recognized carbon stars.

The majority of He-burning stars are clustered in a Red Clump around $I \simeq 21.3$ and $V - I \simeq 0.9$, but a significant number of RR Lyrae is also present and a sparse tail of BHB stars is clearly visible at $V - I \leq 0.4$. The sparse plume of stars between $I \sim 21$ and $I \sim 19.5$, at $V - I \simeq 0.8$ probably hosts the high-mass tail of He-burning stars of the galaxy. One of the two Anomalous Cepheid contained in our catalogue lies at the tip of this feature, in agreement with the above hypothesis. According to the Galactic model by Robin et al. (2003) the total number of foreground Milky Way stars sampled by our field in the color and magnitude ranges displayed in Fig. 1 is $\simeq 21$, with only three foreground stars falling into the region of the CMD populated by the above described plume.

2.1.1 A new RR Lyrae variable

The package we used to produce the above described master frames (ISIS Alard 1999) is aimed at the search of variable stars by mean of a very efficient image subtraction technique (see, for example Cacciari, Bellazzini & Colucci

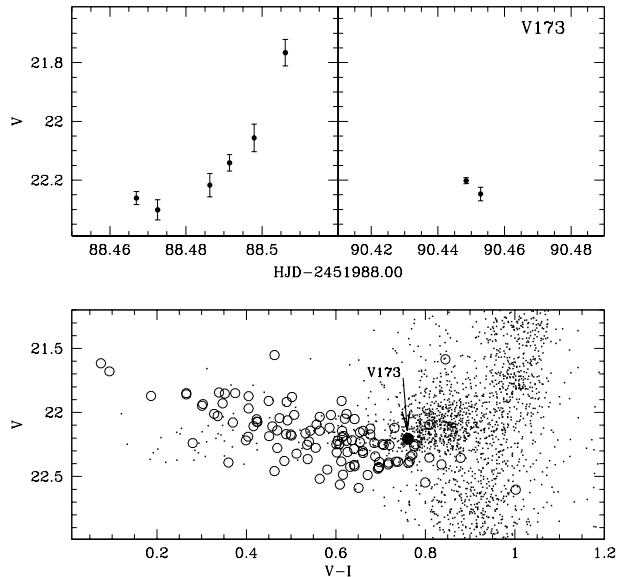


Figure 2. Upper panels: Temporal light variations of the newly identified candidate RR Lyrae star V173. The position of V173 is marked by a filled circle in the CMD shown in the lower panel. Open circles are the RR Lyrae identified from Siegel & Majewski (2000).

2002; Kaluzny et al. 2001; Clementini et al. 2004). Just to verify the performance of the code in difficult conditions (i.e., very sparse time series and typical target just ~ 1 mag brighter than the limiting magnitude of the photometry) we applied the whole image subtraction process to the eight V images from which we obtained our master frame. We identified a list of 14 bona-fide variables with detected variations larger than 0.1 mag in the considered lapse of time. Thirteen of them were variables included in the catalogue of Siegel & Majewski (2000), 12 ab type RR Lyrae and 1 RRc. The fourteenth identified variable is not included in Siegel et al.'s catalogue but the partial light curve we obtained (Fig. 2, upper panel) indicates that it is a real variable star. The large amplitude (> 0.5 mag) and its position in the CMD (shown in the lower panel of Fig. 2) suggest a preliminary classification as a RRab. Following the numbering by Siegel & Majewski (2000) we dub this variable V173. Its coordinates are $(RA_{2000} ; Dec_{2000}) = (11^h 13^m 23.74^s ; 22^\circ 07' 21.7'')$.

2.2 Artificial Stars Experiments

To quantify the effects of the data reduction process on our photometry we performed a set of artificial stars experiments. We followed exactly the procedure described in Bellazzini et al. (2002) and we refer the interested reader to that paper for any detail. The artificial stars were extracted from a LF similar to the observed one, with the additional requirement that they must lie on the average ridge line representing the observed RGB. We limited the artificial stars experiments to RGB stars with $I \leq 22.0$. The stars were added (~ 100 at a time to avoid any spurious modification of the actual crowding conditions) to the master frames and

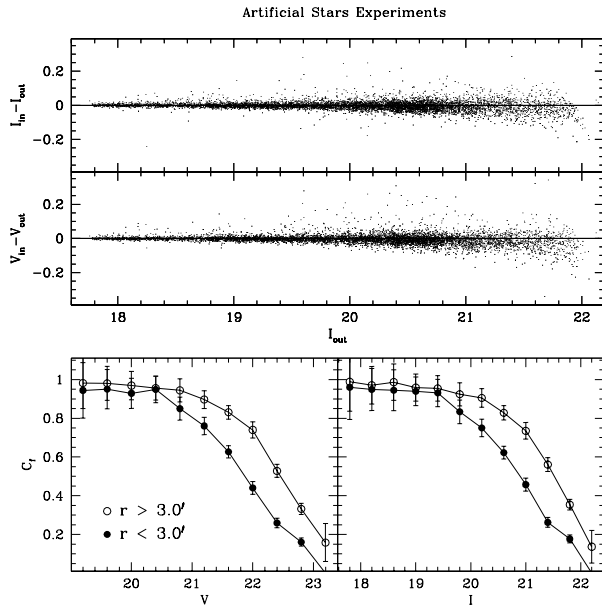


Figure 3. Results of the artificial stars experiments. Upper panels: differences between input and output magnitudes as a function of output magnitude I_{out} . Lower panels: the completeness factor (C_f , see Bellazzini et al. 2002, 2004b) as a function of V and I magnitudes. The effects of the variation of the completeness with the distance from the center of the galaxy are shown by the different behaviour of $C_f(V)$ and $C_f(I)$ in the region within $3'$ from the center (filled circles) and outside $3'$ from the center (empty circles).

the whole process of data reduction was repeated at any run. A total of $\gtrsim 10^4$ artificial stars have been added and processed on the V and I master frames.

The difference between input and output magnitudes, shown in the upper panels of Fig. 3, confirms that the photometric errors are quite small and the degree of blending cannot affect our analyses. The total completeness of the sample (Fig. 3, lower panels) is larger than 80% for $I(V) \lesssim 20.0(21.0)$ and drops below 50% for $I(V) \gtrsim 21.0(22.0)$. The increasing of stellar crowding toward the center of the galaxy produces a significant radial variation of the completeness. The two curves plotted in the lower panels of Fig. 3 show the behaviour of $C_f(V)$ and $C_f(I)$ in the regions within $3'$ from the center (filled circles) and outside $3'$ from the center (empty circles). The spatial variation of the completeness cannot affect any of the results and analyses reported in the following, with the only possible exception of the radial population gradient presented in Sect. 5, below (see the same Sect. 5 for discussion).

3 THE DISTANCE TO LEO II

3.1 Detection of the TRGB

The use of Tip of the Red Giant Branch (TRGB) as a standard candle is now a mature and widely used technique to estimate the distance to galaxies of any morphological type (see Lee et al. 1993a; Madore & Freedman 1995, 1998; Walker 2003, for a detailed description of the

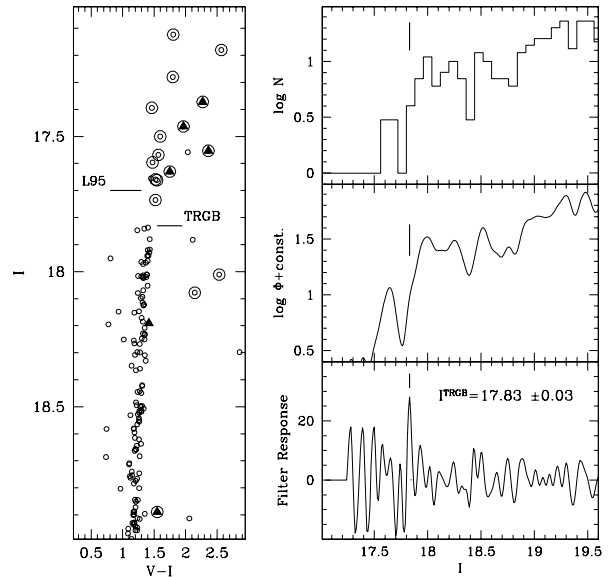


Figure 4. TRGB detection in Leo II. The logarithmic LF of the upper portion of the RGB is shown as an ordinary histogram (upper right panel) and as a generalized histogram (middle right panel, see Laird et al. 1988). The lower right panel shows the Sobel's filter response to the LF. In all panels the thick line marks the position of the TRGB. Left panel: the TRGB level found by us (TRGB) and by Lee (1995) (L95) are reported on the CMD. The symbols are the same as in Fig. 1.

method, recent reviews and applications). The underlying physics is well understood (Madore & Freedman 1998; Salaris, Cassisi & Weiss 2003) and the observational procedure is operationally well defined (Madore & Freedman 1995). The key observable is the sharp cut-off occurring at the bright end of the RGB Luminosity Function (LF) that can be easily detected with the application of an edge-detector filter (Sobel filter, Madore & Freedman 1995; Sakai, Madore & Freedman 1996) or by other (generally parametric) techniques (see, for example Mendez et al. 2002; McConnachie et al. 2004). The necessary condition for a safe application of the technique is that the observed RGB LF should be well populated, with more than ~ 100 stars within 1 mag from the TRGB (Madore & Freedman 1995; Bellazzini et al. 2002). The present sample is at the limit of this requirement, having $N_{\star} = 106$ stars within one magnitude from the detected TRGB (see below). In Sect. 3.3 we will provide additional evidence supporting the robustness of our TRGB detection.

The detection of the TRGB is displayed in Fig. 4. The cut-off of the RGB LF is clearly evident and it is easily detected by the Sobel's filter at $I^{TRGB} = 17.83 \pm 0.03$, where the reported uncertainty is the Half Width at Half Maximum of the peak of the filter response.

The only previous published estimate of I^{TRGB} for Leo II is from (Lee 1995, hereafter L95) who found $I^{TRGB} = 17.7 \pm 0.2$. While formally consistent with our measure, within the errors, the CMD shown in the left panel of Fig. 4 suggests that the TRGB level identified by L95 is too bright, probably due to the influence of the AGB population on his

LF. In this regard, it has to be considered that our field cover an area that is double with respect to L95 and that our sample collects 30% more stars than that of L95, down to $I = 22.0$.

3.2 Metallicity

In Fig. 5 the observed RGB of Leo II is compared with the template ridge lines of the globular clusters NGC 6341, NGC 6205 and NGC 288, taken from the set adopted by Bellazzini et al. (2003). It is immediately clear that the bulk of Leo II RGB stars is enclosed within the ridge lines of NGC 6341 ($[Fe/H]_{CG} = -2.16$; $[Fe/H]_{ZW} = -2.24$; $[M/H] = -1.95$) and of NGC 6205 ($[Fe/H]_{CG} = -1.39$; $[Fe/H]_{ZW} = -1.65$; $[M/H] = -1.18$)⁴.

We derived individual photometric estimates of the metallicity in the different scales for 165 RGB stars having $M_I < -2.5$ by interpolating on the grid of templates ridge lines, as done in Bellazzini et al. (2002, 2003) and Galleti, Bellazzini & Ferraro (2004). From the obtained distributions we derived robust estimates of the average metallicity and of the standard deviation. The median and the average of all the considered distributions differ by just $\lesssim 0.03$ dex, indicating that the average values are not driven by few outlier points but are truly representative of the bulk of the distributions. The final estimates of the mean metallicity and of the distance modulus (see Sect. 3.3, below) have been obtained by an iterative process, adopting $M_I^{TRGB} = -4.05$ as initial guess (see Galleti, Bellazzini & Ferraro 2004). The process converged immediately to the final values because the dependence of M_I^{TRGB} on metallicity is essentially null in the range of metallicity around $[M/H] \sim -1.5$. In the following of this section we shortly compare our average metallicities with previous estimates found in the literature.

- *ZW scale*: we obtain $\langle [Fe/H]_{ZW} \rangle = -1.91$ and $\sigma = 0.22$ dex in excellent agreement with Lee (1995), Demers & Irwin (1993) and Siegel & Majewski (2000). The agreement with Mighell & Rich (1996) is less satisfying but the difference of their estimate to all the others (0.3 dex) is not a reason of serious concern. Moreover, these authors sampled the very central region of the galaxy, where the average metallicity of the stars may be intrinsically higher with respect to outer regions (see Sect. 5, below).

- *CG scale*: we obtain $\langle [Fe/H]_{CG} \rangle = -1.74$ and $\sigma = 0.30$ dex, within 0.2 dex of the spectroscopical estimate by Bosler et al. (2004). Our metallicity distribution is also broadly similar to that obtained by these authors (for instance, the range is $-2.4 \leq [Fe/H]_{CG} \leq -1.2$ while Bolster et al. find $-2.32 \leq [Fe/H]_{CG} \leq -1.26$), suggesting that our photometric metallicities are quite reliable in the present case.

- *global metallicity scale*: $\langle [M/H] \rangle = -1.53$ and $\sigma = 0.30$

⁴ $[M/H]$ is the *global metallicity*, a parameter that includes the contribution of Iron and of the α -elements (O, Mg, Ti, Si, etc.), hence it is a more suitable indicator of the global metal content to relate with the observed properties of stars and stellar populations and for comparisons with theoretical models (see Salaris, Chieffi & Straniero 1993; Ferraro et al. 1999; Bellazzini et al. 2004a,b, for discussion and references).

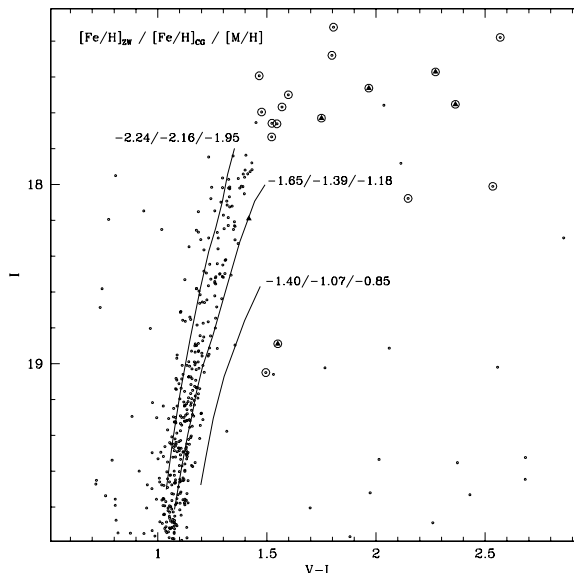


Figure 5. Comparison of the observed RGB of Leo II (assuming $(m - M)_0 = 21.84$ and $E(B - V) = 0.02$) with the ridge lines of the templates adopted by (Bellazzini et al. 2003). The plotted ridge lines are from NGC 6341, NGC 6205 and NGC 288, from left to right, respectively. The label reports the metallicity of the templates in the ZW, CG and global metallicity scales. The symbols are the same as in Fig. 1.

dex. Taking into account the contribution of photometric errors to the derived metallicity dispersion as done in Bellazzini et al. (2002); Galleti, Bellazzini & Ferraro (2004), we estimate that the $1 - \sigma$ intrinsic dispersion is $\simeq 0.25$ dex, in good agreement with Lee (1995); Demers & Irwin (1993); Mighell & Rich (1996); Bosler et al. (2004).

3.3 The distance modulus of Leo I

To obtain the distance modulus of Leo II we adopt the calibration of M_I^{TRGB} as a function of the global metallicity ($[M/H]$) recently provided by Bellazzini et al. (2004a)

$$M_I^{TRGB} = 0.258[M/H]^2 + 0.676[M/H] - 3.629 \pm 0.12. \quad (1)$$

At the mean metallicity $[M/H] = -1.53$ (as derived in Sect. 3.2, above), the resulting distance modulus is $(m - M)_0 = 21.84$.

This estimate is affected by the combination of uncertainties coming from different sources, i.e. : the estimate of apparent magnitude of the TRGB ($\sigma = 0.03$ mag, plus the $\sigma = 0.02$ mag uncertainty on the zero-point of the absolute photometric calibration), the calibrating relation ($\sigma = 0.12$ mag, see Bellazzini et al. 2004a), the reddening ($\sigma = 0.01$ mag), and the assumed global metallicity ($\sigma = 0.3$ dex). Properly propagating all these uncertainties we finally obtain $(m - M)_0 = 21.84 \pm 0.13$, corresponding to a heliocentric distance $D = 233 \pm 15$ Kpc.

This result is consistent with all previous estimates within the uncertainties quoted by the various authors, typically ± 0.2 mag, but is outside of their formal range $21.55 \leq (m - M)_0 \leq 21.78$. However it has to be considered

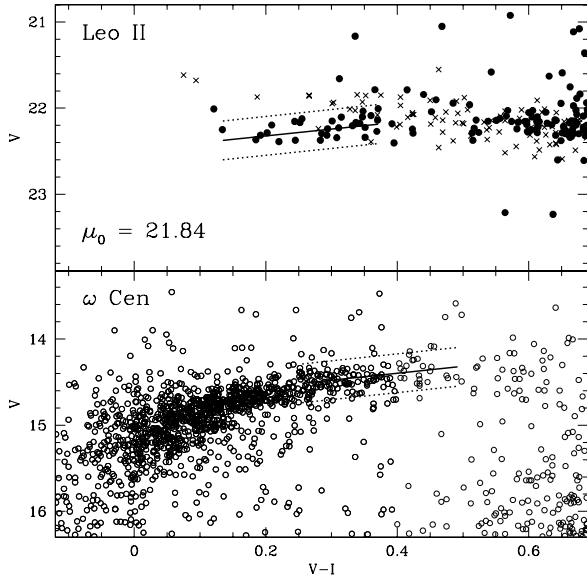


Figure 6. Upper panel: the HB of Leo II. The thick continuous line is the ridge line of the BHB stars, while the dotted lines enclose the whole BHB distribution. Lower panel: the Leo II BHB ridge lines are compared with the observed BHB stars of ω Cen (data from Pancino et al. 2000) after correction for the differences in reddening and distance modulus between the two stellar systems. The adoption of the distance modulus derived from the TRGB provides an excellent match of the BHB sequences.

that (a) all previously determined distance moduli are tied to different RR Lyrae-based distance scales and (b) the uncertainty in the absolute magnitude of the adopted standard candle was taken as null in all cases. Hence (a) part of the difference may be due to systematic differences between the adopted distance scales and (b) the true $1 - \sigma$ uncertainties of previous estimates should be of order $\sim \pm 0.25/0.3$ mag, to compare with our ± 0.13 which includes all the possible sources of errors.

As said in Sect. 3.1, the number of bright RGB stars of Leo II contained in our sample is just above the limit for a safe detection of the TRGB. To verify the robustness of the above derived distance modulus to sampling effects we compare the luminosity of the BHB of Leo II with that of the cluster that provide the fundamental zero-point of our calibration of the TRGB method (e.g. ω Centauri, see Bellazzini, Ferraro & Pancino 2001; Bellazzini et al. 2004a). For a favorable circumstance the metallicity of the main population of ω Cen ($[M/H] \simeq -1.4$, see Sollima et al. (2004)) is very similar to the average metallicity of Leo II. In the upper panel of Fig. 6 we show the ridge line of the mean level of the BHB of Leo II (continuous line) as well as the lines enclosing the whole BHB distribution (dotted lines). In the lower panel of Fig. 6 these ridge lines are compared to the observed BHB of ω Cen (from Pancino et al. 2000) adopting $(m - M)_0^{Leo II} = 21.84$ and $(m - M)_0^{\omega Cen} = 13.70$, $E(B - V)^{\omega Cen} = 0.11$, according to Bellazzini et al. (2004a). It can be readily appreciated that the TRGB distance modulus carries the HBs of Leo II and ω Cen essentially to a

perfect match, providing further support to the reliability of our distance estimate.

4 THE RGB BUMP(S)

The RGB bump is the effect of a well known phase of the RGB evolution of low mass stars (see Iben 1968; Fusi Pecci et al. 1990, and references therein). When the H-burning shell of a RGB star encounters the chemical discontinuity left behind by the maximum penetration of the convective envelope, the luminosity of the star has a slight drop. When the shell adapts at the new environment the luminosity grows again, but at a different pace than before. As a result the stars pile-up at this stage, producing a *bump* in the RGB LF and the slope of the LF changes above the bump, because of the change in the evolutionary rate. The RGB bump has been extensively studied in globular clusters (see Fusi Pecci et al. 1990; Zoccali et al. 1999; Ferraro et al. 1999, - hereafter F99 - and references therein), but it has been detected in dwarf galaxies only in recent times (Majewski et al. 1999; Bellazzini et al. 2001, 2002; Monaco et al. 2002; Lee et al. 2003). Monaco et al. (2002) and Bellazzini (2004) provided direct evidence that significant constraints on the age and metal content of dSph galaxies can be obtained from the study of this observational feature.

Majewski et al. (1999) and Bellazzini et al. (2001) interpreted the detection of two bumps on the RGB LF as indication of the presence of two distinct populations in Sculptor and Sextans, respectively. A preliminary detection of a double RGB bump in Leo II, from the same dataset studied here, has been presented in Bellazzini (2004). Lee et al. (2003) argued against this interpretation, proposing that the brightest of the two bumps found in these galaxies is due to the AGB clump instead (Gallart & Bertelli 1998).

In the attempt of minimizing the effects of any possible AGB Clump on the RGB LF we carefully selected our sample of RGB stars. The adopted selection is shown in the upper-right panel of Fig. 7. Note that the sparse cluster of stars located at $V \simeq 21.3$ and $V - I \simeq 0.9$ that may be identified with the AGB clump of the main population of Leo II has been excluded from the selection, as well as the bluest stars of the whole sequence, which may presumably have the highest degree of contamination from AGB stars. In spite of that, the right-panels of Fig. 7 show that two significant bumps are detected on the RGB of Leo II. The main bump (B1) is at $V^{bump} = 21.76 \pm 0.05$, the less pronounced one (B2) is at $V^{bump} = 21.35 \pm 0.05$. While B1 can be straightforwardly interpreted as the RGB bump of the dominant stellar population of Leo II, the nature of B2 is more uncertain. We combined Eq. 7 and Eq. 6.6 of F99 (obtained from well studied galactic globulars) to derive a relation for the difference in V magnitude of the AGB clump and the RGB Bump (ΔV_{bump}^{AGB}) as a function of the global metallicity:

$$\Delta V_{bump}^{AGB} = -0.360[M/H]^2 - 1.772[M/H] - 2.283 \pm 0.09. (2)$$

The difference in magnitude between B2 and B1 ($\Delta V_{B2-B1} = -0.41 \pm 0.07$) is in excellent agreement with the predictions of Eq. 2 for $[M/H] \simeq -1.5$, i.e. $\Delta V_{bump}^{AGB} =$

-0.43 ± 0.09^5 . This result seems to favor the interpretation of B2 as a feature associated with the AGB clump of the same population that generated the RGB bump B1. On the other hand, as shown in Fig. 7, our RGB selection should have removed most of the AGB clump stars from the considered sample. Hence the possibility that B2 is a genuine secondary RGB Bump cannot be excluded at the present stage. Given this uncertain interpretation we drop any further discussion of B2 in the following analysis, which is focused on B1 instead. Larger photometric samples and dedicated theoretical modeling of the luminosity functions in the AGB phase are needed to achieve a clearer view of the problem of double bumps in the context of composite stellar populations.

In the lower-left panel of Fig. 7 we compare the absolute V magnitude of B1 with three isochrones in the M_V^{bump} vs. $[M/H]$ plane obtained from Eq. 3 of F99 (see Monaco et al. 2002; Bellazzini 2004). According to F99, the bulk of the Galactic globular clusters is comprised between the 16 Gyr and the 12 Gyr isochrones, in this plane. Hence, the position of B1 indicates that the main population of Leo II is more than 4 Gyr younger than the typical Galactic globular, in excellent agreement with the results of Mighell & Rich (1996), obtained from the analysis of the Main Sequence Turn Off (MSTO) of Leo II. The inclusion in the plot of the main RGB bump of ω Cen (see S04) provides again a real case to compare with: the difference in M_V^{bump} between this cluster and Leo II(B1) is at the $\geq 2 - \sigma$ level. It has to be recalled that the age difference between the Main Population (MP) of Leo II and classical globular clusters would be lower than what read from the lower-left panel of Fig. 7 if the Helium abundance of Leo II - MP is higher than that of the clusters (see S04 and references therein).

5 A POPULATION GRADIENT IN LEO II

Population gradients are a common feature in dSph galaxies (see Harbeck et al. 2001, - hereafter H01 - and references therein). In all the cases in which a radial gradient has been found, the sense is invariably that the most metal-rich/young populations are more centrally concentrated than the metal-poor/older ones. Since the HB is the evolutionary phase in which low-mass stars display the maximum sensitivity to metallicity and age (as well as to a number of other physical parameters, see Fusi Pecci et al. 1993), in most cases the gradients have been detected using HB stars as tracers (H01, Bellazzini et al. 2002).

In Fig. 8 the cumulative radial distributions of Red Clump (RC) stars and of BHB+RR Ly stars are compared. The plot shows that the usual kind of radial gradient is present also in Leo II: RC stars are significantly more centrally concentrated than the BHB+RR Ly stars. A Kolmogorov-Smirnov test quantifies the probability that the two samples are extracted from the same parent distribution to less than 0.01 %. While the two considered populations have essentially the same average V magnitude (see Fig. 2, above), the BHB+RR Ly stars are ~ 0.5 mag fainter than the RC

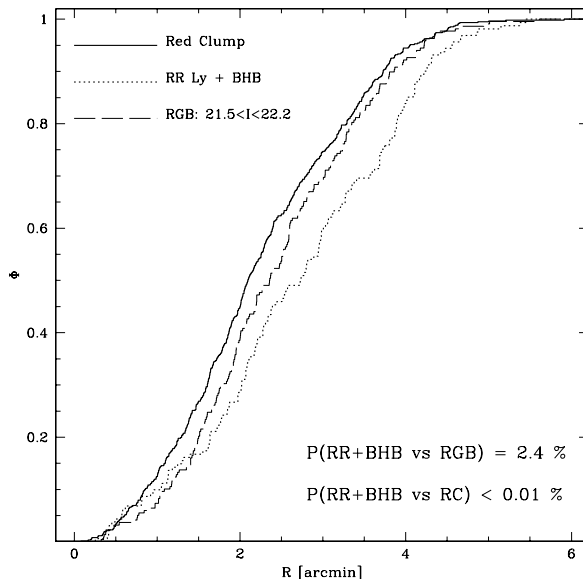


Figure 8. Cumulative radial distributions of Red Clump stars (continuous line), RR Lyrae and Blue Horizontal Branch stars (dotted line), and RGB stars fainter than the RC (long dashed line, adopted as a control sample). The probability that the samples are extracted from the same parent radial distribution - according to a Kolmogorov-Smirnov test - is reported in the lower right angle of the plot.

in I, hence the BHB+RR Ly sample may be slightly less complete than the RC one. Is it possible that this fact, coupled with the radial variation of the completeness discussed in Sect. 2.2, has originated a spurious difference in the distribution of BHB+RR Ly and RC stars? To test this hypothesis we plot in Fig. 8 also the distribution of RGB stars fainter than the RC (Faint RGB). Note that this sample should be less complete than the BHB+RR Ly one since its members are fainter in V while having I magnitudes similar to BHB+RR Ly. Hence, if the detected population gradient is due to the radial variations of the completeness, the Faint RGB sample should display a radial distribution even more extended than the BHB+RR Ly. Fig. 8 shows that this is not the case: the distribution of Faint RGBs is much more similar to that of RC stars than to the distribution of BHB+RR Ly. Therefore, the observed difference between the radial distributions of RC and BHB+RR Ly stars is not due to completeness effects but it traces a real population gradient.

It is very likely that both age and metallicity variations are at the origin of the effect. However, since RC stars dominates the HB population of Leo II it is reasonable to associate them with the main population of the galaxy, whose mean age is $\simeq 9$ Gyr, according to Mighell & Rich (1996), while RR Lyrae and BHB stars should be associated with older populations (up to age=14 Gyr Mighell & Rich 1996). In this framework the age would be the main driver of the gradient.

⁵ At odds with the results of the preliminary analysis shown in Bellazzini (2004). The difference is entirely due to the fact that in that analysis we assumed $[M/H] \simeq -1.7$, instead of $[M/H] \simeq -1.5$, as adopted here.

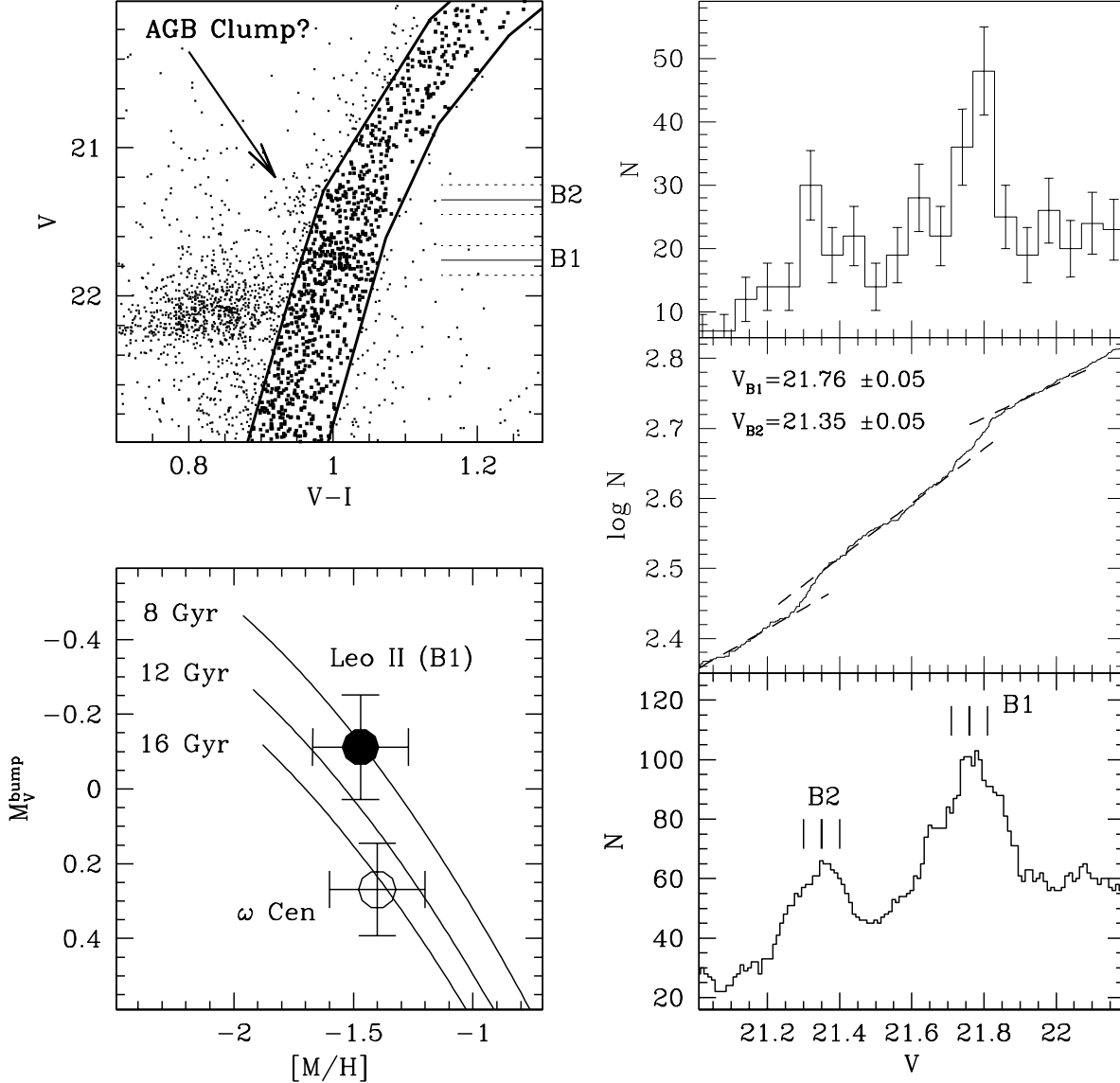


Figure 7. Upper-left panel: the selection of RGB stars adopted to derive the LF. The selected RGB stars are the heavier dots enclosed within the RGB-shaped box. Upper-right panel: the LF as an ordinary histogram, with error bars. Middle-right panel: the LF as a logarithmic cumulative distribution. Lower panel: the LF as a smoothed histogram with bin width of 0.16 mag and incremental step of 0.01 mag. The position of the bumps and the associated uncertainty ranges are indicated by thick and thin vertical segments, respectively. Lower-left panel: The absolute V magnitude of the RGB bump of Leo II (B1, filled circle) and of the main population of ω Cen (open circle, see S04) are compared with isochrones of different ages derived from Eq. 3 of F99.

6 CONCLUSIONS

We have provided a clean and accurate detection of the I magnitude of the TRGB of Leo II. Adopting the average metallicity we derived from the same data by comparison with templates RGB ridge lines, and the calibration of M_I^{TRGB} as a function of the global metallicity ($[M/H]$) provided by Bellazzini et al. (2004a) we have obtained a new estimate of the distance modulus of Leo II, $(m - M)_0 = 21.84 \pm 0.13$, corresponding to a distance $D = 233 \pm 15$ Kpc.

The effects of all the possible sources of uncertainty have been taken into account.

Two significant bumps have been detected in the LF of the RGB of Leo II. The fainter bump (B1) has been identified as the RGB bump of the main population of the galaxy, while the brighter one (B2) may be due to stars belonging to the AGB clump of the same population or may be a secondary RGB bump, associated with another population of the galaxy. The luminosity of the main bump (B1) indicates that the main population of Leo II is several ($\gtrsim 4$) Gyr

younger than the typical Galactic globular clusters, in good agreement with the estimates obtained from the photometry of the MSTO by Mighell & Rich (1996). This result suggests that useful indications on the age may be obtained from the RGB bump also for distant stellar systems whose MSTO is out of the reach of currently available telescopes (see also Monaco et al. 2002; Bellazzini 2004, and S04).

A significant population gradient has been detected for the first time in this galaxy: the BHB and RR Lyrae stars have a more extended radial distribution with respect to stars in the Red Clump. Age differences are proposed as the main driver of the observed gradient.

ACKNOWLEDGMENTS

Based on observations made with the Italian Telescopio Nazionale Galileo (TNG) operated on the island of La Palma by the Centro Galileo Galilei of the INAF (Istituto Nazionale di Astrofisica) at the Spanish Observatorio del Roque de los Muchachos of the Instituto de Astrofisica de Canarias. This research is part of the Thesis of Degree of N. Gennari (Bologna University). This research is partially supported by the Italian Ministero dell'Università e della Ricerca Scientifica (MURST) through the COFIN grant p. 2002028935-001, assigned to the project *Distance and stellar populations in the galaxies of the Local Group*. The financial support of the Agenzia Spaziale Italiana (ASI) is also acknowledged. Y. Momany is acknowledged for providing his unpublished photometry of Leo II that we used to check our photometric calibration. We are grateful to an anonymous Referee for his/her useful comments and indications. Part of the data analysis has been performed using software developed by P. Montegriffo at the INAF - Osservatorio Astronomico di Bologna. This research has made use of data products from the 2MASS, a joint project of Univ. of Massachusetts, IPAC/CIT funded by NASA and NSF. This research has made use of data products from the Guide Star Catalogue, produced at STScI. This research has made use of NASA's Astrophysics Data System Abstract Service.

REFERENCES

- Alard, C., 1999, A&A, 343, 10
 Alard, C., 2000, A&AS, 144, 363
 Azzopardi, M., Lequeux, J., & Westerlund, B.E., 1985, A&A, 144, 388
 Bellazzini, M., Ferraro, F.R., Pancino, E., 2001, ApJ, 556, 635
 Bellazzini, M., Ferraro, F.R., & Pancino, E., MNRAS, 327, L15
 Bellazzini, M., Ferraro, F.R., Origlia, L., Pancino, E., Monaco, L., Oliva, E., 2002, AJ, 124, 3222
 Bellazzini, M., Cacciari C., Federici L., Fusi Pecci F., Rich M., 2003, A&A, 405, 867
 Bellazzini M., Ferraro F.R., Sollima A., Pancino E., Origlia L., 2004a, A&A, 424, 199 (B04)
 Bellazzini M., Gennari N., Ferraro F.R., 2004b, MNRAS, 379
 Bellazzini M., 2004, in Stars in Galaxies, M. Bellazzini, A. Buzzoni and S. Cassisi Eds., Mem. SAIt, 75, 118
 Bosler T.L., Smecker-Hane T.A., Cole A., Stetson P.B., 2004, in Origin and Evolution of the Elements, A. McWilliam and M. Rauch Eds., <http://www.ociw.edu/ociw/symposia/series/symposium4/proceedings.htm>
 Cacciari, C., 1999, in Harmonizing Cosmic Distance Scales in a Post-HIPPARCOS Era, D. Egret and A. Heck Eds., ASP, S. Francisco, ASP Conf. Ser., vol. 167, p. 140
 Cacciari C., Bellazzini M., Colucci S., 2002, in Extragalactic Star Clusters, IAU Symposium 207, D. Geisler, E.K. Grebel, and D. Minniti Eds., San Francisco: Astronomical Society of the Pacific, p. 168
 Carretta E., & Gratton R.G., 1997, A&AS, 121, 95 (CG)
 Explanatory Supplement to the 2MASS All-Sky Data Release, <http://www.ipac.caltech.edu/2mass/releases/allsky/doc/explsup.html>
 Clementini G., Corwin T.M., Carney B.W., Sumerel A.N., 2004, AJ, 127, 938
 Dean J.F., Warren P.R., Cousins A.W.J., 1978, MNRAS, 183, 569
 Demers S., Irwin M.J., 1993, MNRAS, 261, 657
 Demers S., Harris W.E., 1983, AJ, 88, 329
 Ferraro F.R., Messineo M., Fusi Pecci F., De Palo M.A., Straniero O., Chieffi A., Limongi M., 1999, AJ, 118, 1738 (F99)
 Fusi Pecci, F., Ferraro, F.R., Crocker, D.A., Rood, R.T., & Buonanno, R., 1990, A&A, 238, 95
 Fusi Pecci, F., Ferraro, F.R., Bellazzini M., Djorgovski S.G., Piotto G., Buonanno, R., 1993, AJ, 105, 1145
 Iben, I., Jr., 1968, Nature, 220, 143
 Galletti S., Bellazzini M., Ferraro F.R., 2004, A&A, 423, 925
 Gallart C., Bertelli G., 1998, in The Magellanic Clouds and other dwarf galaxies, T. Richtler and J.M. Braun Eds., Aachen: Shaker Verlag, Berichte aus der Astronomie Series, p. 249
 Harbeck D., et al., 2001, AJ, 122, 3092 (H01)
 Harrington R.G., Wilson A.G., 1950, PASP, 62, 118
 Kaluzny J., Olech A., Stanek K.Z., 2001, AJ, 121, 1533
 Laird, J.B., Rupen, M.P., Carney, B.W., Latham, D.W., AJ, 96, 1908
 Lee M.G., Freedman W.L., Madore B.F., 1993a, ApJ, 417, 553 (LFM93)
 Lee M.G., 1995, AJ, 110, 1155
 Lee M.G., et al., 2003, AJ, 126, 2840
 Madore, B.F., Freedman, W.L., 1995, AJ, 109, 1645 (MF95)
 Madore, B.F., Freedman, W.L., 1998, in Stellar Astrophysics for the Local Group, A. Aparicio, A. Herrero and F. Sanchez Eds., Cambridge: Cambridge University Press, p. 305
 Majewski, S.R., Siegel, M.H., Patterson, R.J., Rood, R.T., 1999, ApJ, 520, L33
 Mateo, M., 1998, ARA&A, 36, 435
 McConnachie, A.W., Irwin, M.J., Ferguson, A.M.N., Ibata, R.A., Lewis, G.F. & Tanvir, N. 2004, MNRAS, 350, 243
 Mendez, B., Davis, M., Moustakas, J., Newman, J., Madore, B.F., Freedman, W.L., 2002, AJ, 124, 213
 Mighell K.J., Rich R.M., 1996, AJ, 111, 777
 Momany Y., 2000, Ph.D. Thesis, Padova University
 Monaco L., Ferraro F.R., Bellazzini M., Pancino E., 2002, ApJ, 578, L47
 Monaco L., Bellazzini M., Ferraro F.R., Pancino E., 2004, MNRAS, 353, 874

- Pancino E., Ferraro F.R., Bellazzini M., Piotto G., Zoccali M., 2000, *ApJ*, 534, L83
- Renzini, A., Fusi Pecci, F., 1988, *Ann. Rev. A&A*, 26, 199
- Robin A.C., Reylé S., Derrière S., Picaud S., 2003, *A&A*, 409, 523
- Sakai, S., Madore, B.F, Freedman W.L., 1996, *ApJ*, 461, 713 (SMF96)
- Salaris, M., Chieffi, A., Straniero O., 1993, *ApJ*, 414, 580
- Salaris, M., Cassisi, S., Weiss, A., 2003, *PASP*, 114, 375
- Schechter, P.L., Mateo, M., Saha, A., 1992, *PASP*, 105, 1342
- Schlegel, D., Finkbeiner, D. & Davis, M., 1998, *ApJ*, 500, 525
- Siegel M.H., Majewski S., 2000, *AJ*, 120, 284
- Sollima A., Ferraro F.R., Pancino E., Bellazzini M., 2004, *MNRAS*, in press
- Stetson, P. , 2000, *PASP*, 112, 925
- Vogt S.S., Mateo M., Olszewski E.W., Keane M.J., 1995, *AJ*, 109, 151
- Zinn, R., West, M.J., 1984, *ApJS*, 55, 45
- Walker, A.R., 2003, in *Stellar Candles for the Extragalactic Distance Scale*, D. Alloin and W. Gieren Eds., Springer, *Lecture Notes in Physics*, in press, (astro-ph/0303011)
- Zoccali M., Cassisi S., Piotto G., Bono G., Salaris M., 1999, *ApJ*, 518, L49